Available online at www.sciencedirect.com
ScienceDirect
International Journal of Heat and Fluid Flow 29 (2008) 1164–1173
International Journal of HEAT AND FLUID FLOW
www.elsevier.com/locate/ijhff

Buoyancy convection in a square cavity with mutually orthogonal heat generating baffles

A.K. Abdul Hakeem, S. Saravanan *, P. Kandaswamy

UGC-DRS Center for Fluid Dynamics, Department of Mathematics, Bharathiar University, Coimbatore 641 046, India

Received 25 October 2007; received in revised form 10 January 2008; accepted 16 January 2008
Available online 20 March 2008

Abstract

A two-dimensional numerical solution for buoyancy induced convection in a square cavity with discretely heat generating baffles is presented in the context of cooling of electronic equipments. The walls of the cavity are subjected to either isothermal temperature or outward isoflux. The Grashof number and Prandtl number are fixed at 10^6 and 0.71, respectively. The effects of different locations of the baffles are reported in terms of streamlines and temperature contours. The results obtained clearly show that the fluid flow and temperature fields strongly depend on location of the baffles. The movement of either the horizontal or vertical plate produces no significant changes in the overall heat transfer rate except when one of them is wall mounted in the presence of isothermal cavity walls. In the case of isoflux cavity walls the overall heat transfer rate gets suppressed for the upward movement of the horizontal baffle and enhanced for the horizontal movement of the vertical baffle in the core region of the cavity. When one of the baffles moves closer to a cavity wall thermal boundary layer is formed and hence conduction becomes dominant in between them in the case of isothermal cavity walls. But in general the presence of isoflux cavity walls arrests crowding of isotherms.

Keywords: Buoyancy; Cavity; Heat generation; Isothermal; Isoflux

1. Introduction

Buoyancy convection in an enclosure induced by internal energy sources has attracted many researchers, due to its practical engineering applications, such as exchange of heat between building and environment, heat removal from electrical and electronic equipments, food processing, nuclear reactor design and control of flows in rooms due to thermal energy sources. Natural convection cooling is desirable because it does not require an energy source, such as a forced air fan and it is maintenance free and safe. Despite significantly lower values of convection heat transfer coefficient, cooling by natural convection using air is preferred, in numerous electronic cooling applications because of its low cost, inherent reliability, simplicity and noiseless method of thermal control.

The geometries that arise in engineering applications, however, are more complicated than a simple horizontal or vertical cavity. Many studies have been performed on natural convection in cavities with various obstacles placed inside in the form of partitions, partial baffles and square bodies. They revealed that these kinds of obstructions would change the characteristics of flow and heat transfer in the horizontal and vertical cavities. Natural convection in a differentially heated square cavity with a horizontal thin fin attached to the hot wall was studied by Bilgen (2005). He reported that *Nu* is an increasing function of *Ra* and a decreasing function of fin length and relative conductivity ratio. The heat transfer may be suppressed up to 38% by choosing appropriate thermal and geometrical fin parameters. Numerical study of natural convection of air in a differentially heated cubical enclosure with a thick fin

* Corresponding author. Tel.: +91 422 2422222x415; fax: +91 422 2425706.
E-mail addresses: abdulhakeem6@yahoo.co.in (A.K. Abdul Hakeem), sshravan@lycos.com (S. Saravanan), pgkswamy@yahoo.co.in (P. Kandaswamy).

0142-727X/$ - see front matter © 2008 Elsevier Inc. All rights reserved.
doi:10.1016/j.ijheatfluidflow.2008.01.015

Nomenclature

d_i	distance between center of cavity and baffles (m)	β	volumetric coefficient of expansion of fluid (1/K)
D_i	dimensionless distance	θ	temperature (K)
g	acceleration due to gravity (m/s^2)	ψ	stream function (m^2/s)
Gr	Grashof number $= g\beta\nabla TL^3/\nu_f^2$	μ	dynamic viscosity of fluid (Pa s)
$J(\psi,\zeta)$	Jacobian of Ψ,ζ with respect to X_1, X_2	ν	kinematic viscosity $= \mu/\rho$ (m^2/s)
L	length of the cavity (m)	ρ	density of fluid (kg/m^3)
Nu	local Nusselt number $= \partial T/\partial X_i$	τ	dimensionless time
Nu_{wall}	average Nusselt number $= \int_{-0.5}^{0.5} Nu\, dX_i$	ω	vorticity (1/s)
P	pressure (Pa)	Ψ	dimensionless stream function
Pr	Prandtl number $= \nu_f/\alpha_f$	ζ	dimensionless vorticity
t	time (s)		
T	dimensionless temperature	*Subscript*	
v_i	velocity (m/s)	i	1, 2
V_i	dimensionless vertical velocity	c	cold
x_i	cartesian coordinate (m)	h	hot
X_i	dimensionless cartesian coordinate		
α	thermal diffusivity (m^2/s)		

placed vertically in the middle of the hot wall was made by Frederik (2007). A three-dimensional convective circulation was generated, in which the cold flow sweeps the fin faces and the hot wall, with low flow blockage. Abdullatif and Chamkha (2006) analyzed natural convection in a square cavity fitted with an inclined heated thin fin of arbitrary length attached to the hot wall. They reported that thin fin inclination and length have significant effects on the average Nusselt number of the heated wall including the fin of the enclosure. Oztop et al. (2004) have reported natural convection in a cavity with a thin heated plate built in vertically or horizontally and found that heat transfer is enhanced by about 20% when the plate is located vertically. Very recently, laminar natural convection heat transfer in a tilted rectangular enclosure containing vertically situated hot plates has been numerically investigated by Altac and Kurtul (2007). They found that the mean Nusselt number increases with tilt angle up to 22.5° where it reaches a maximum and then declines for all Rayleigh numbers. Dagtekin and Oztop (2001) have dealt with the heat removal from two heated vertical partitions of different heights placed on the bottom of a cavity and observed the enhancement of heat transfer with an increase in both spacing between the two partitions and height of the partitions.

For the past few years considerable research has also been performed to extract heat from hotter bodies contained in closed cavities. Ha et al. (1999) investigated the unsteady natural convection process in three different fluids such as sodium, air and water contained in a differentially heated square cavity within which a centered, square heat conducting body generates heat. They studied the effects of Rayleigh number, Prandtl number, thermal conductivity ratio, heat capacity ratio and the temperature difference ratio on the transient streamlines, isotherms and average Nusselt numbers at the hot and cold walls. Bessaih and Kadja (2000) numerically simulated conjugate turbulent natural convection air cooling of three heated ceramic components mounted on a vertical adiabatic channel. The effects on cooling of spacing between the heated electronic components and of the removal of heat input in one of the components were determined. Ha et al. (2002) solved the problem of two-dimensional and unsteady natural convection in a horizontal square enclosure with a square body located at the center between the bottom hot and top cold walls. The body was maintained with adiabatic and isothermal boundary conditions for different Rayleigh numbers. Lee and Ha (2005) investigated natural convection in a horizontal layer of fluid with a conducting body in the interior, using an accurate and more efficient Chebyshev spectral collocation approach. They reported that convection is relatively weak and Nu calculated at the bottom hot wall depends on the variation of thermal conductivity ratio for $Ra < 10^4$. When $Ra \geqslant 10^5$ convection became more dominant and Nu did not much depend on variation of thermal conductivity ratio. Very recently, natural convection in a differentially heated square cavity with uniform internal heat generation and with an isothermal partition attached on the bottom wall was studied numerically by Oztop and Bilgen (2006). They reported that heat transfer is reduced more effectively when the partition is closer to the hot or cold wall. Natural convection in an enclosure containing a tilted heated square cylinder has been studied numerically by Kumar and Dalal (2006). Their results indicated that the uniform wall temperature heating is quantitatively different from the uniform heat flux heating.

Most of the previous studies reported on natural convection in a cavity containing obstacles deal with square heat conducting body placed at the center with and without heat generation. Heat transfer in an enclosure with two

mutually orthogonal heated plates has received limited attention though such configurations are encountered in microelectronics industry. Papanicolaou and Jaluria (1994) and Icoz and Jaluria (2004) have considered such cases in their design and optimization of cooling systems for electronic equipments. During the last decade, engineers in the electronic industry were looking for the best way to cool electronic components. However, efficient cooling cannot be achieved without understanding the heat transfer from each component and determining the flow and thermal fields. It is in response to this need that simulations of cooling of electronic equipments have become an active area today, for experimental and computational research. Hence the present numerical study deals with the effect of various locations of two mutually orthogonal discretely heat generating baffles (DHGB) placed in a square cavity and also results were compared with isothermal heated baffle (ITHB). This type of configuration enables to study the relative location of a heating element with respect to the other in sealed cavities which provide some additional information to the basic design.

2. Mathematical analysis

The physical model and coordinate system of the problem under consideration are illustrated schematically in Fig. 1. It is a two-dimensional square cavity of sides of length L containing two mutually orthogonal heat generating baffles of the length $L/2$. The baffles are treated as line sources and generate heat at a uniform rate q'''. The horizontal and vertical baffles are at distances d_1 and d_2 from the center O of the cavity, respectively. The vertical and horizontal walls are isothermally maintained at a constant temperature θ_c for ITBC (isothermal boundary condition) or subjected to a uniform outward heat flux q'' for IFBC (isoflux boundary condition). The cartesian co-ordinates (x_1, x_2) with the corresponding velocity components (v_1, v_2) are chosen. The gravity $\bar{g}$ acts downwards parallel to the x_1 direction.

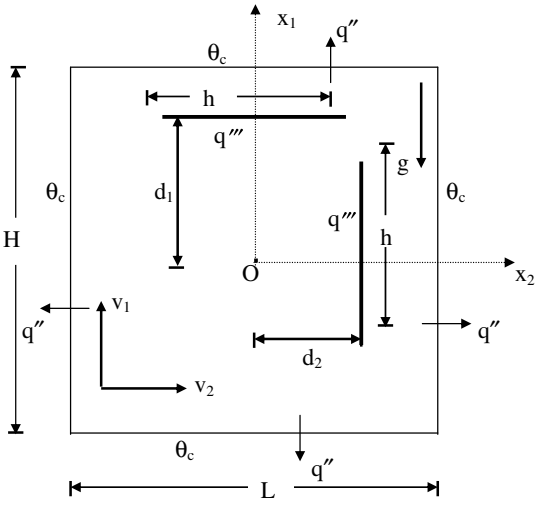

Fig. 1. Physical configuration.

The analysis is based on the two-dimensional assumption. All the fluid properties are taken to be constant except the density in the buoyancy term following the Boussinesq approximation.

The conservation governing equations for fluids are as follows:

$$\frac{\partial v_1}{\partial x_1}+\frac{\partial v_2}{\partial x_2}=0 \tag{1}$$

$$\frac{\partial v_1}{\partial t}+v_1\frac{\partial v_1}{\partial x_1}+v_2\frac{\partial v_1}{\partial x_2}=-\frac{1}{\rho_0}\frac{\partial p}{\partial x_1}+\nu\nabla^2 v_1-g\beta(\theta-\theta_c) \tag{2}$$

$$\frac{\partial v_2}{\partial t}+v_1\frac{\partial v_2}{\partial x_1}+v_2\frac{\partial v_2}{\partial x_2}=-\frac{1}{\rho_0}\frac{\partial p}{\partial x_2}+\nu\nabla^2 v_2 \tag{3}$$

$$\frac{\partial \theta_f}{\partial t}+v_1\frac{\partial \theta_f}{\partial x_1}+v_2\frac{\partial \theta_f}{\partial x_2}=\alpha_f\nabla^2\theta_f \tag{4}$$

$$\frac{\partial \theta_b}{\partial t}=\alpha_b\nabla^2\theta_b+\frac{q'''}{\rho C_p} \tag{5}$$

The appropriate initial and boundary conditions are

$$t=0: \quad v_i=0; \quad \theta=\theta_c; \quad \text{at} \quad -\frac{L}{2}\leqslant x_i\leqslant\frac{L}{2} \tag{6}$$

$$t>0: \quad v_i=0; \quad \theta=\theta_c; \quad \text{at} \quad x_i=\pm\frac{L}{2} \quad \text{for ITBC} \tag{7}$$

$$t>0: \quad v_i=0; \quad \frac{\partial\theta}{\partial x_i}=\pm q''; \quad \text{at} \quad x_i=\pm\frac{L}{2} \quad \text{for IFBC} \tag{8}$$

$v_i=0$ on the baffles

$\theta=\theta_b$ at fluid/body interface

The vorticity–stream function formulation is used here to get rid of the pressure field and reduce the number of equations. Accordingly the non-dimensional form of the governing equations takes the form

$$\frac{\partial\zeta}{\partial\tau}+J(\psi,\zeta)=Gr\frac{\partial T}{\partial X_2}+\nabla^2\zeta \tag{9}$$

$$\frac{\partial T_f}{\partial\tau}+J(\psi,T_f)=\frac{1}{Pr_f}\nabla^2 T_f \tag{10}$$

$$\frac{\partial T_b}{\partial\tau}=\frac{1}{Pr_f}\left[\alpha\nabla^2 T_b+\frac{1}{\rho C_p}\right] \tag{11}$$

$$\nabla^2\psi=-\zeta \tag{12}$$

The dimensionless variables of the above equations are defined as

$$X_i=\frac{x_i}{L}, \quad D_i=\frac{d_i}{L}, \quad \tau=\frac{t}{L^2/\nu_f}, \quad T=\frac{\theta-\theta_c}{\Delta T},$$

$$\Psi=\frac{\psi}{\nu} \quad \text{and} \quad \zeta=\frac{\omega L^2}{\nu}.$$

The dimensionless parameters are

$$Gr=\frac{g\beta\Delta TL^3}{\nu_f^2}, \quad Pr=\frac{\nu_f}{\alpha_f}, \quad \alpha=\frac{\alpha_b}{\alpha_f}, \quad \rho C_p=\frac{(\rho C_p)_b}{(\rho C_p)_f},$$

$$\kappa=\frac{\kappa_b}{\kappa_f}$$

where

$$\Delta T = \begin{cases} \theta_h - \theta_c & \text{for ITBC} \\ q'' L/\kappa_f & \text{for IFBC} \\ q''' L^2/\kappa_f & \text{for DHGB} \end{cases} \quad (13)$$

The dimensionless form of initial and boundary conditions are as follows

$$\tau = 0;\ \frac{\partial \psi}{\partial X_i} = 0;\ T = 0;\ \text{at}\ -\frac{1}{2} \leqslant X_i \leqslant \frac{1}{2} \quad (14)$$

$$\tau > 0;\ \frac{\partial \psi}{\partial X_i} = 0;\ T = 0;\ \text{at}\ X_i = \pm\frac{1}{2}\ \text{for ITBC} \quad (15)$$

$$\tau > 0;\ \frac{\partial \psi}{\partial X_i} = 0;\ \frac{\partial T}{\partial X_i} = \pm 1;\ \text{at}\ X_i = \pm\frac{1}{2}\ \text{for IFBC} \quad (16)$$

$$\frac{\partial \psi}{\partial X_i} = 0;\ \text{on the baffles}$$

$$T = T_b\ \text{at fluid/baffle interface}$$

In order to measure heat transfer rate in the cavity, it is necessary to define wall Nusselt numbers at the four walls as $Nu_{wall} = \int_{-0.5}^{0.5} Nu\, dX_i$, where the local Nusselt number

$$Nu = \begin{cases} \frac{\partial T}{\partial X_i} & \text{for ITBC and} \\ \frac{1}{T} & \text{for IFBC} \end{cases} \quad (17)$$

The average Nusselt number $\overline{Nu}$ is then calculated by averaging the wall Nusselt numbers at the four walls. If one of the heat generating baffles lies on a cavity wall, only the remaining part of that wall is taken in calculating Nu_{wall}.

3. Numerical technique and validation tests

The motion of the fluid governed by the continuity, momentum and energy equations are solved numerically using the finite difference method with a regular cartesian space grid. An alternating direction implicit (ADI) technique and successive over relaxation (SOR) method are employed to solve the discretized equations as reported in Saravanan and Kandaswamy (2000). The results obtained by the code developed were validated against those of Zhong et al. (1985) and Oztop et al. (2004) for ITBC and Sharif and Mohammad (2005) for IFBC (see Fig. 2b). In both the cases we observe a good agreement. In order to determine a proper grid size for this study, a grid independency test was conducted for $Gr = 10^6$, $Pr = 0.71$ and $D_1 = D_2 = 0$. Five different grids $41 \times 41, 61 \times 61, 81 \times 81, 101 \times 101$ and 121×121 were chosen. The maximum value of the stream function of the primary eddy ($|\Psi|_{max}$) was used as a sensitivity measure of the accuracy of the solution. Fig. 2 shows that the two grids 101×101 and 121×121 give nearly identical results. Hence considering both the accuracy and the computational time, the computations were all performed with a 101×101 grid.

4. Results and discussion

Buoyancy convection in a square cavity induced by two mutually orthogonal heat generating baffles is investigated numerically with the surrounding walls maintained at either isothermal or isoflux conditions. The simulations were carried out for fixed values of $Gr = 10^6$ and $Pr = 0.71$ corresponding to air. The present study deals with the heat transfer characteristics due to heat generating baffles placed at different locations in the cavity. The effects of dimensionless thermal diffusivity α, solid–fluid thermal conductivity ratio and thermal boundary conditions have already been studied in detail Bessaih and Kadja (2000), Ha et al. (2002), Oztop and Bilgen (2006), Kumar and Dalal (2006). Hence in the present study we fixed the values of dimensionless thermal diffusivity, α as 1 and ρC_p as

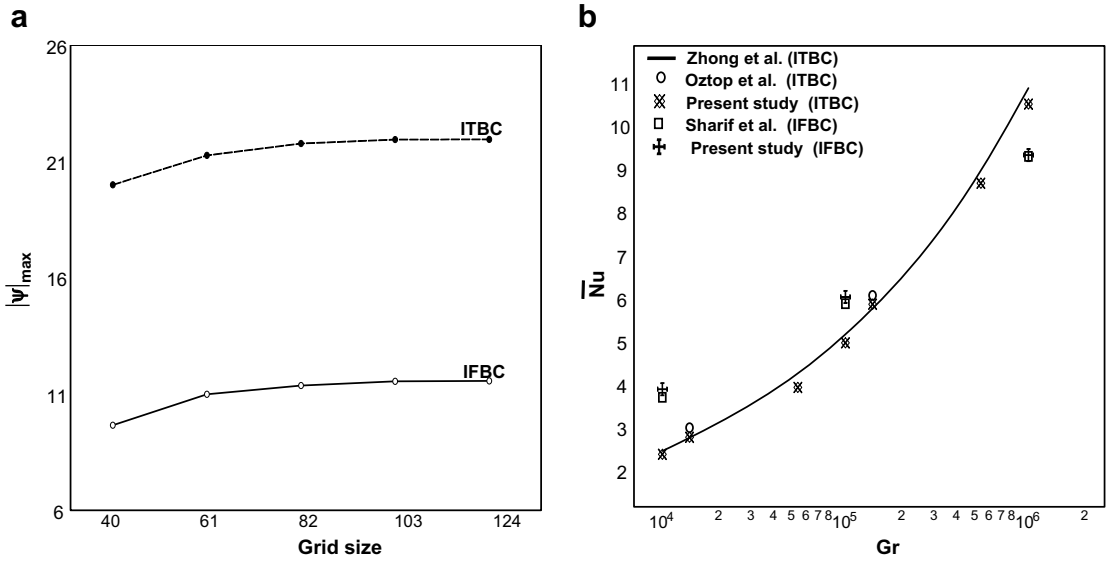

Fig. 2. (a) $|\Psi|_{max}$ as a function of the grid size. (b) Correlation of present numerical results with others.

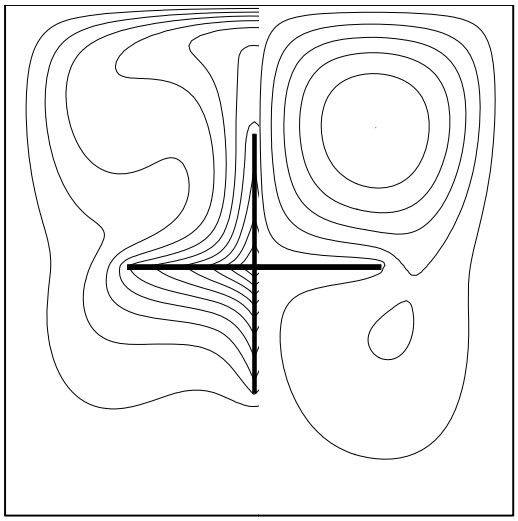

T_{max}= 1.561 and $|\Psi|_{max}$ = 23.124

Fig. 3. Isotherm and streamline for $D_1 = D_2 = 0.0$.

0.0007 as in Ha et al. (1999). Throughout the study we have plotted both isotherms and streamlines for ten and five equally spaced values between T_{min} and T_{max} for temperature and zero and $|\Psi|_{max}$ for the stream function, respectively. We study the effects of different locations of the horizontal and vertical baffles by fixing $D_2 = 0$ and $D_1 = 0$, respectively. When $D_2 = 0.0$, the problem is symmetric about $X_2 = 0$. Hence we have given both streamlines and isotherms in a single plot.

4.1. Isothermal boundary condition (ITBC)

Fig. 3 shows the isotherms and streamlines when both the plates are located at the center of the cavity ($D_1 = D_2 = 0$). Two counter rotating circulation patterns with strong primary eddies above and weak secondary eddies below the baffles are formed as anticipated. The primary eddy becomes slightly more stronger and the secondary eddy becomes slightly more weaker compared to the ITHB case.

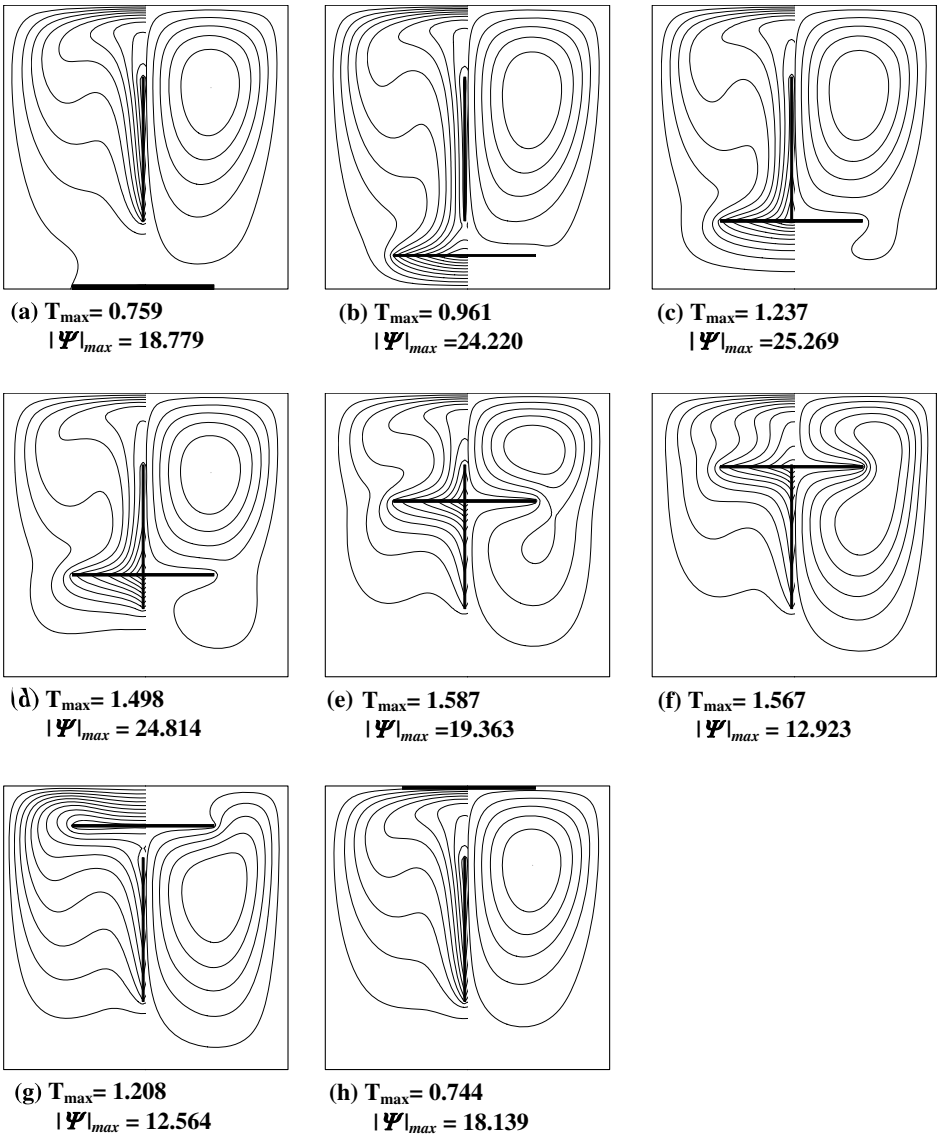

Fig. 4. Isotherms and streamlines for ITBC when $D_2 = 0.0$ and $D_1 = 0.5, 0.375, 0.25, 0.125, -0.125, -0.25, -0.375, -0.5$.

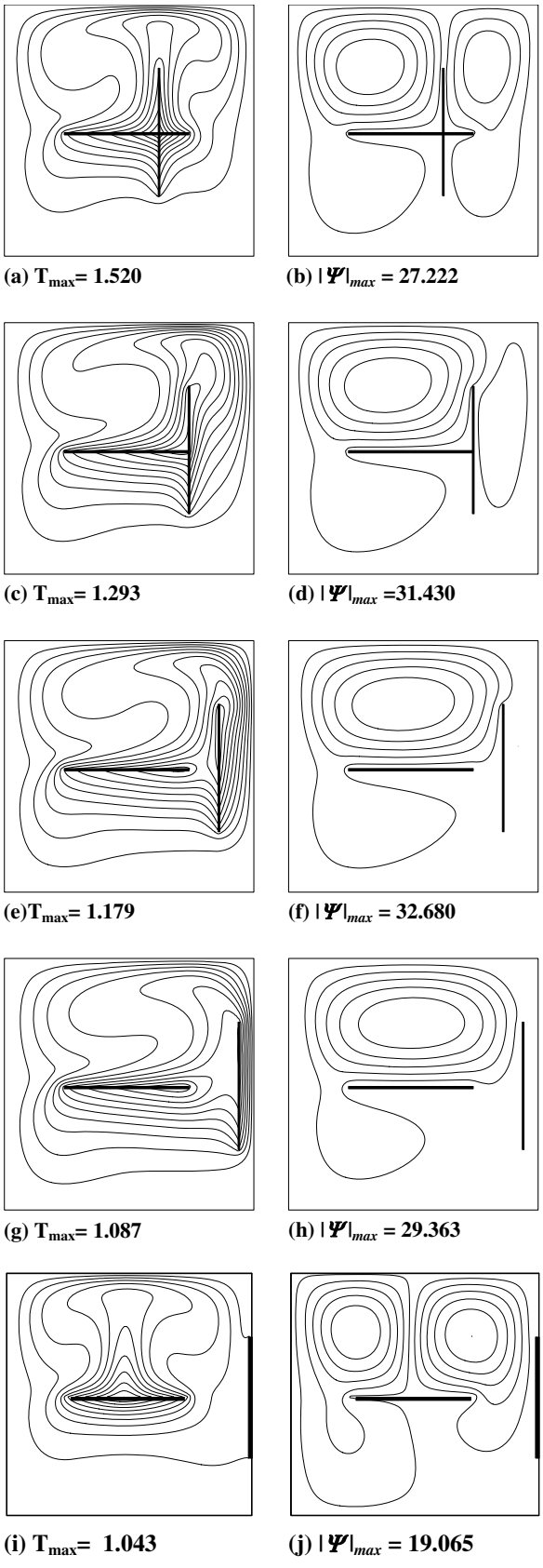

Fig. 5. Isotherms and streamlines for ITBC when $D_1 = 0.0$ and different values of $D_2 = 0.125, 0.25, 0.375, 0.5$.

The changes in isotherms and streamlines for various positions of the horizontal baffle are displayed in Fig. 4. The upward movement of the horizontal baffle in the core region ($-0.25 \leqslant D_1 \leqslant 0.25$) diminishes the active region in which the primary eddies are formed and hence develops secondary eddies below the baffle. This increases the wall Nusselt numbers below the horizontal baffle and hence the overall Nusselt number experiences an increase (Fig. 6a). This behaviour is in contradiction to the ITHB case in which a decrease in $\overline{Nu}$ was observed. When the horizontal baffle comes closer to the horizontal walls ($D_1 = \pm 0.375$) conduction effect becomes important in between them. When the horizontal baffle is top wall mounted the resulting heat transfer characteristics behave as if it is absent. When it is bottom wall mounted its contribution in inducing convection cell is meager. Thus sudden drops are seen in $\overline{Nu}$ for the wall mounted cases. This in turn brings down the changes in $\overline{Nu}$ when the

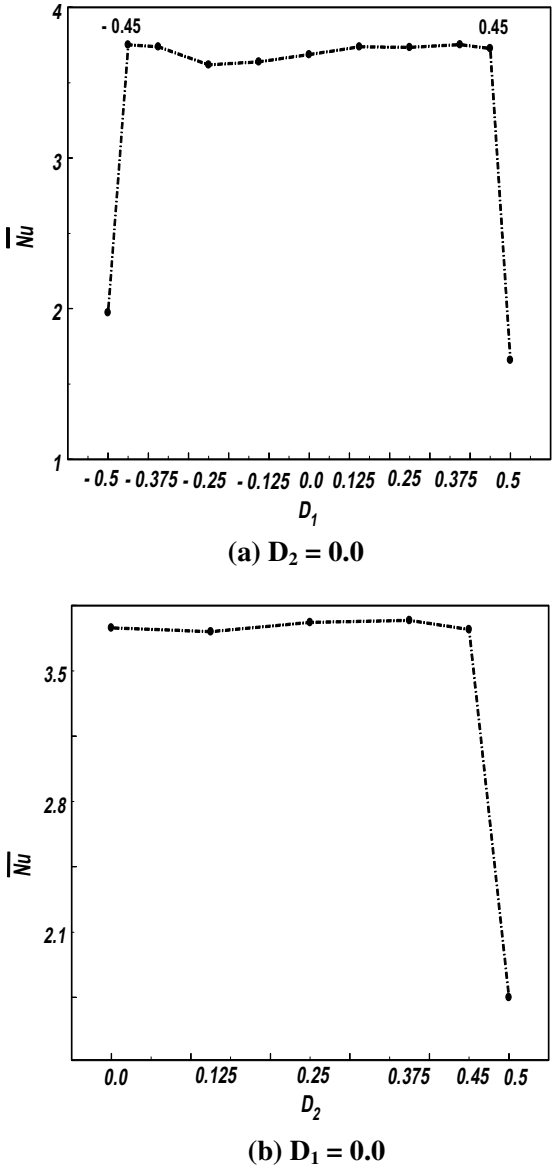

Fig. 6. $\overline{Nu}$ for different values of D_1 and D_2 for ITBC.

horizontal baffle lies within the cavity. Thus only small changes in the overall heat transfer rate are seen for intermediate values of D_1.

The temperature and stream function contours for various positive values of D_2 corresponding to the vertical baffle movement are shown in Fig. 5. As D_2 increases from zero, the right convection cell gets suppressed gradually and the anti-clockwise rotating left cell starts filling the entire cavity with a corresponding increase in its $|\Psi|_{max}$. When $D_2 = 0.5$ the vertical baffle becomes almost inactive in inducing the buoyancy force. A thermal induced by the horizontal baffle at the center of the cavity generates two counter rotating convection cells which descend along the two vertical cavity walls. Hence a sudden fall in $\overline{Nu}$ is noticed in Fig. 6b. This behaviour is different from the ITHB case. In ITHB case both the baffles were jointly responsible for the formation of an anti-clockwise rotating cell filling the entire cavity.

A sudden reduction in the buoyancy force responsible for the development of convection is observed when both the baffles are wall mounted (Fig. 7). These are clearly seen from the values of T_{max} and $|\Psi|_{max}$. The isotherms do not penetrate the cavity well so that it can make a favourable situation for the development of better convection. It is worth mentioning here that a favourable isothermal pattern was produced in the ITHB case also.

4.2. Isoflux boundary condition (IFBC)

In the presence of a uniform outward heat flux applied at the cavity walls the isotherms get attracted towards the cavity walls. This behaviour introduces a favourable temperature gradient for the enhancement of convection below the baffle as well. Unlike ITBC IFBC blocks the formation of thermal boundary layers when one of the baffles comes closer to the cavity walls. The isotherms and streamlines corresponding to $D_1 = D_2 = 0$ are shown in Fig. 8. We observe a comparatively stronger flow at the lower half of the cavity than that in the ITBC case. We also observe a reduction in $|\Psi|_{max}$, corresponding to the strength of the primary eddy compared to ITBC.

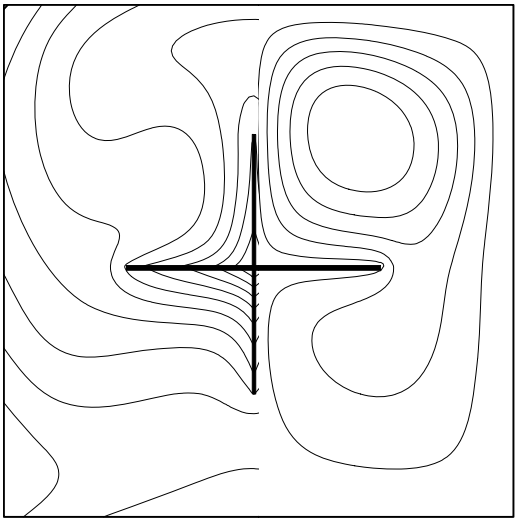

T_{max}= 18.482 and $|\Psi|_{max}$ =14.092

Fig. 8. Isotherm and streamline for $D_1 = D_2 = 0.0$.

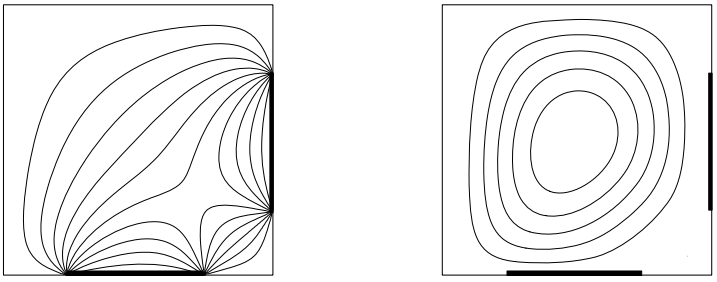

T_{max}= 0.201 **$|\Psi|_{max}$ = 0.421**

(a) D_1 = -0.5 and D_2 = 0.5

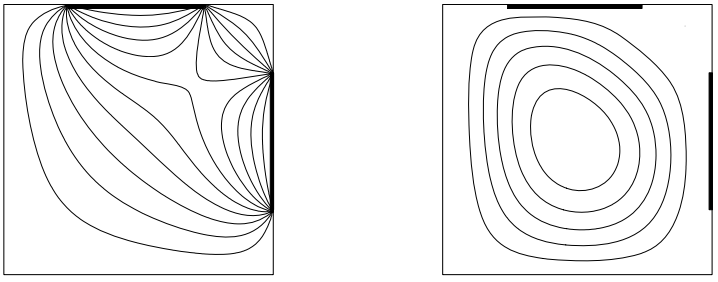

T_{max}= 0.183 **$|\Psi|_{max}$ = 0.146**

(b) $D_1 = D_2 = 0.5$

Fig. 7. Isotherms and streamlines for ITBC.

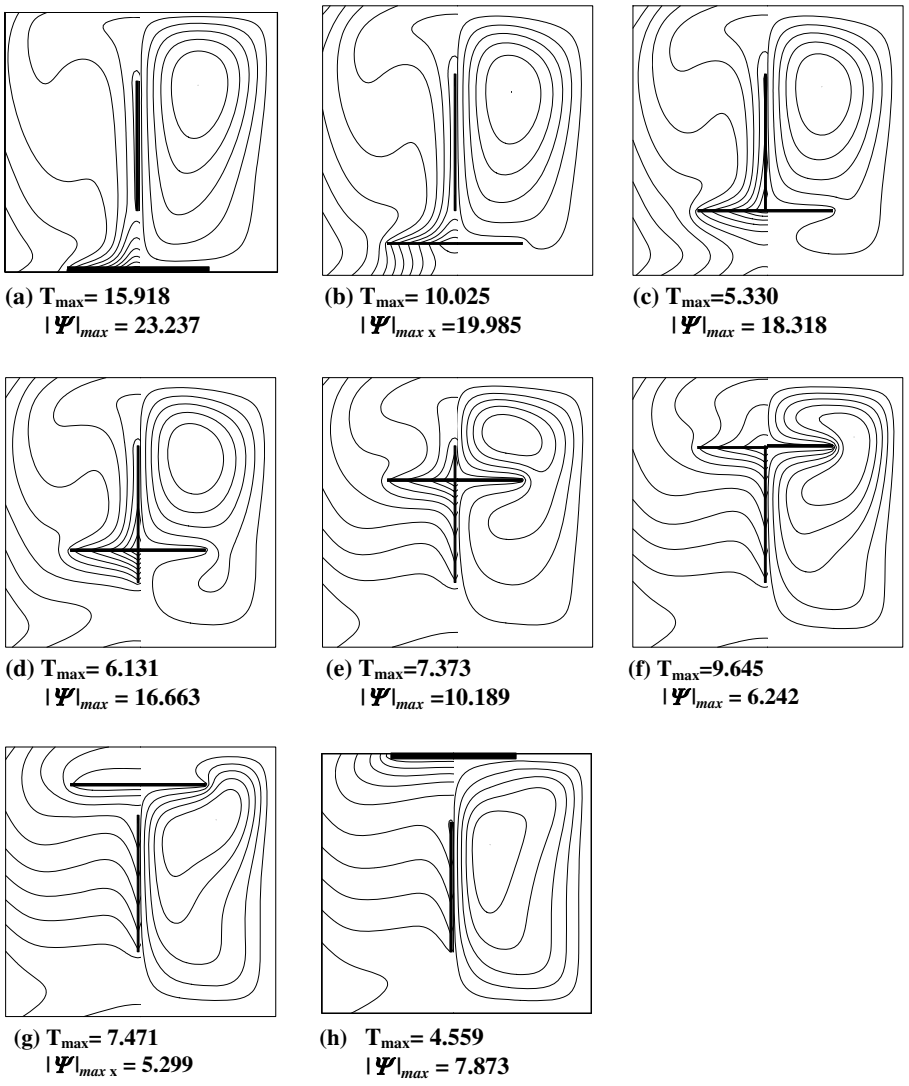

Fig. 9. Isotherms and streamlines when $D_2 = 0.0$ for $D_1 = 0.5, 0.375, 0.25, 0.125, -0.125, -0.25, -0.375, -0.5$.

Figs. 9 and 10 show the effects of D_1 and D_2 on the convective patterns. A closer look at these (for instance Figs. 4h and 9h) shows that the cell centers are attracted towards the vertical baffle. This is due to the presence of outward flux at the cavity walls which removes the heat energy more vigorously and thereby makes the fluid to sink quickly. It is also noticed that as the horizontal baffle moves upwards in the core region $D_1 \times D_2 \in ((-0.25, 0.25) \times (-0.25, 0.25))$ free flow in the upper half of the cavity is blocked and hence a reduction in $|\Psi|_{\max}$ is seen. This is reflected in the $\overline{Nu}$ as a corresponding drop. When the horizontal baffle comes closer and closer to the bottom cavity wall (Fig. 9b) the isotherms in between them looks almost like straight lines. Thus the heat energy from the baffle is transferred to the bottom wall instantaneously showing that the horizontal baffle behaves like a cold wall. Thus a sharp increase in $\overline{Nu}$ is noticed in Fig. 11a for this case. It is interesting to mention that $\overline{Nu}$ reaches its minimum when the horizontal plate is at the position $D_1 = 0.375$ where it reached its maximum in the ITHB case. In the case of ITBC overall heat transfer shoots up when one of the plates comes close to a cavity wall due to the formation of thermal boundary layer. Fig. 11b shows the increasing nature of $\overline{Nu}$ for an increase in D_2 except when $D_2 = 0.5$ corresponding to the wall mounted case. Fig. 12 depicts convective patterns when both the plates are wall mounted. When $D_1 = D_2 = 0.5$ a counter rotating bicellular symmetrical pattern descending at the middle of the cavity is seen. This is a unique phenomenon observed which was not present in ITHB–ITBC, ITBC–IFBC and DHGB–ITBC cases.

5. Conclusion

The effect of different locations of two mutually orthogonal heat generating baffles on buoyancy convection in a

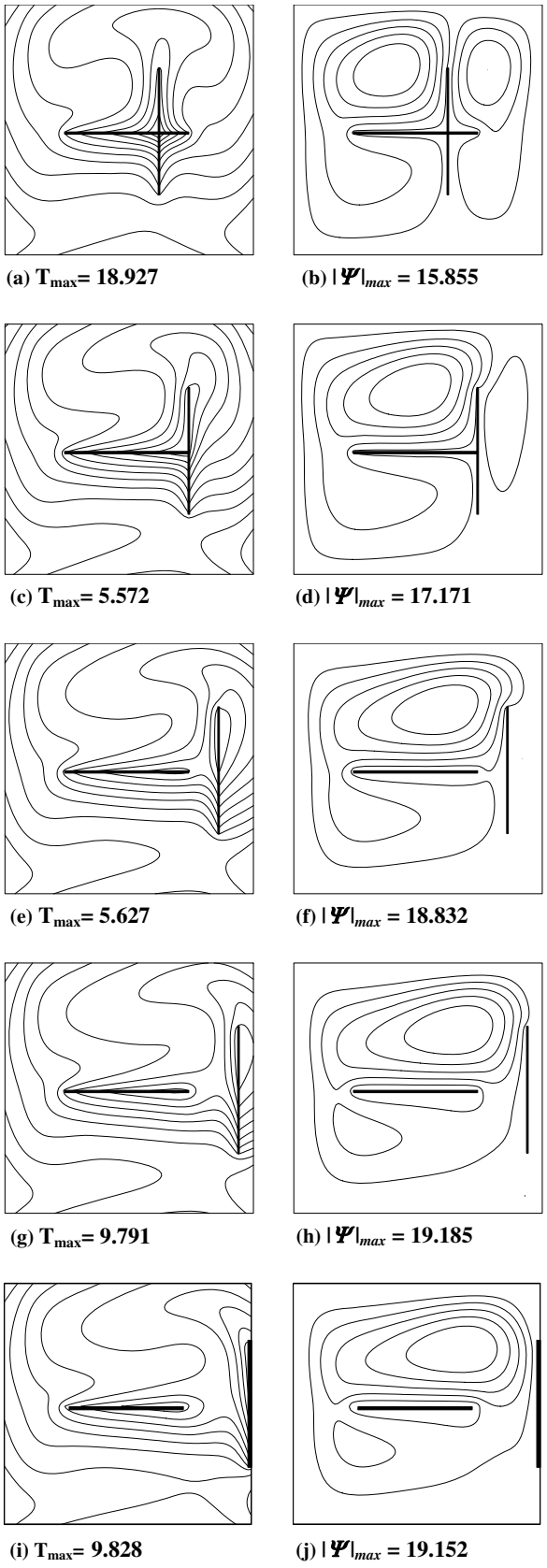

Fig. 10. Isotherms and streamlines for IFBC when $D_1 = 0.0$ and $D_2 = 0.125, 0.25, 0.375, 0.45, 0.5$.

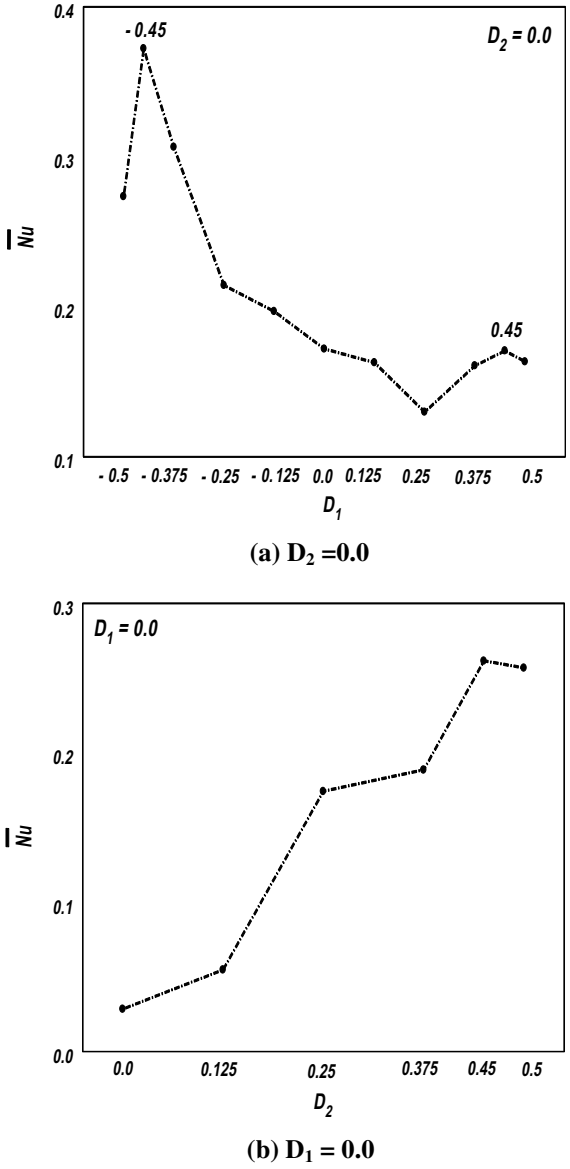

Fig. 11. $\overline{Nu}$ for different values of D_1 and D_2 for IFBC.

square cavity with isothermal or isoflux walls is investigated. The study leads to the following conclusions:

- The movement of either the horizontal or vertical baffle produces no significant changes in the overall heat transfer rate except when one of them is wall mounted in the ITBC case. But significant changes are observed in the IFBC case. The overall heat transfer rate reaches its maximum when either the horizontal baffle is located very close to the bottom wall or the vertical baffle located very close to the side wall.
- In the IFBC case the overall heat transfer rate gets suppressed for the upward movement of the horizontal baffle and enhanced for the horizontal movement of the vertical baffle in the core region.

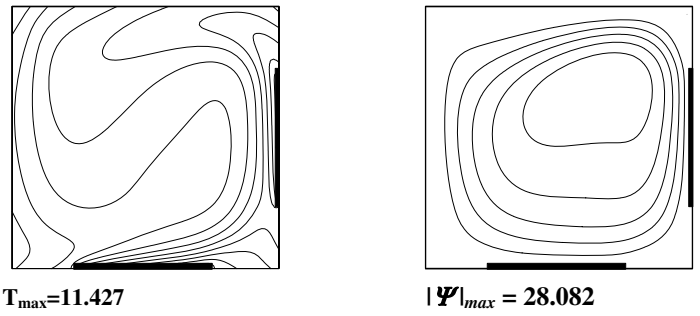

Fig. 12. Isotherms and streamlines for IFBC.

- When one of the baffles moves closer to a cavity wall conduction becomes dominant in between them for the ITBC case. But the presence of IFBC arrests the formation of thermal boundary layer between them which is responsible for the conduction dominated mechanism.
- A drop in overall heat transfer rate is observed whenever one of the baffles is wall mounted. This drop is sharp in the ITBC case.
- In the IFBC case a counter rotating symmetrical bicellular pattern is noticed when the baffles are mounted on the top and side walls.

References

Abdullatif, B.N., Chamkha, A.J., 2006. Effect of a length and inclination of a thin fin on natural convection in a square enclosure. Numer. Heat Transfer A 50, 389–407.

Altac, Z., Kurtul, O., 2007. Natural convection in tilted rectangular enclosures with a vertically situated hot plate inside. Appl. Therm. Eng. 27, 1832–1840.

Bessaih, R., Kadja, M., 2000. Turbulent natural convection cooling of electronic components mounted on a vertical channel. Appl. Therm. Eng. 20, 141–154.

Bilgen, E., 2005. Natural convection in cavities with a thin fin on the hot wall. Int. J. Heat Mass Transfer 48, 3493–3505.

Dagtekin, I., Oztop, H.F., 2001. Natural convection heat transfer by heated partitions within enclosure. Int. Commun. Heat Mass Transfer 28, 823–834.

Frederik, R.L., 2007. Heat transfer enhancement in cubical enclosure with vertical fins. Appl. Therm. Eng. 27, 1585–1592.

Ha, M.Y., Jung, M.J., Kim, Y.S., 1999. A numerical study on transient heat transfer and fluid flow of natural convection in an enclosure with a heat-generating conducting body. Numer. Heat Transfer A 35, 415–434.

Ha, M.Y., Kim, I.K., Yoon, H.S., Yoon, K.S., Lee, J.R., 2002. Two-dimensional and unsteady natural convection in a horizontal enclosure with a square body. Numer. Heat Transfer A 41, 183–210.

Icoz, T., Jaluria, Y., 2004. Design of cooling systems for electronic equipment using both experimental and numerical inputs. ASME J. Electron. Packaging 126, 465–471.

Kumar, D.A., Dalal, A., 2006. A numerical study of natural convection around a square, horizontal, heated cylinder placed in an enclosure. Int. J. Heat Mass Transfer 49, 4608–4623.

Lee, J.R., Ha, M.Y., 2005. A numerical study of natural convection in a horizontal enclosure with a conducting body. Int. J. Heat Mass Transfer 48, 3308–3318.

Oztop, H., Bilgen, E., 2006. Natural convection in differentially heated and partially divided square cavities with internal heat generation. Int. J. Heat Fluid Flow 27, 466–475.

Oztop, H.F., Dagtekin, I., Bahloul, A., 2004. Comparison of position of a heated thin plate located in a cavity for natural convection. Int. Commun. Heat Mass Transfer 31, 121–132.

Papanicolaou, E., Jaluria, Y., 1994. Mixed convection from simulated electronic components at varying relative positions in a cavity. ASME J. Heat Transfer 116, 960–970.

Saravanan, S., Kandaswamy, P., 2000. Natural convection in low Prandtl number fluids with a vertical magnetic field. ASME J. Heat Transfer 122, 602–606.

Sharif, M.A.R., Mohammad, T.R., 2005. Natural convection in cavities with constant flux at the bottom wall and isothermal cooling from the sidewalls. Int. J. Therm. Sci. 44, 865–878.

Zhong, Z.Y., Yang, K.T., Lloyd, J.R., 1985. Variable property effects in laminar natural convection in a square enclosure. ASME J. Heat Transfer 17, 133–138.